SIMULATION OF SEMICONDUCTOR DEVICES AND PROCESSES Vol. 5
Edited by S. Selberherr, H. Stippel, E. Strasser - September 1993

Atomistic Evaluation of Diffusion Theories for the Diffusion of Dopants in Vacancy Gradients

S. List[‡], P. Pichler[‡], and H. Ryssel[‡†]

[‡]Fraunhofer-Institut für Integrierte Schaltungen
Artilleriestraße 12, D-91052 Erlangen, GERMANY
[†]Lehrstuhl für Elektronische Bauelemente, Universtität Erlangen-Nürnberg
Cauerstraße 6, D-91052 Erlangen, GERMANY

Abstract

A new approach is used for the the calculation of transport coefficients for dopants and vacancies from atomic jump frequencies in the presence of dopant or vacancy gradients. Results are shown for the diffusion under vacancy gradients with an attractive potential between the dopant and the defect. It is demonstrated that for a given vacancy gradient not only the absolute value but also the sign of the dopant flux depends on the range of the binding potential.

1. Introduction

Despite large efforts in recent years, the basic diffusion mechanisms are still under discussion. Basically, there are two common formulations of the diffusion equations for dopants including the effects of gradients of the point defect concentrations. According to pair diffusion theories [1], the flux of dopants is predicted in the same direction as the flux of the vacancies. On the other hand, atomistic theories neglecting pair diffusion [2] lead to an opposite direction of the two fluxes. If the dopant flux is written as a function of dopant and vacancy gradient as

$$-\underline{F}_d = \frac{C_v}{C_{site}} \cdot D_d^o \cdot \underline{\nabla} C_d + \alpha \cdot D_d^o \cdot \frac{C_d}{C_{site}} \cdot \underline{\nabla} C_v \tag{1}$$

then the pair diffusion model [1] will lead to $\alpha = 1$ whereas atomistic theories [2] correspond to $\alpha = -1$. In (1), C_d and C_v denote the concentrations of dopants and vacancies, D_d^o is the normalized dopant diffusion coefficient (scaled with the probability of a site to be occupied by a vacancy). Both approaches have to be seen as idealizations and the underlying atomistic mechanisms remain unclear. Therefore the aim of the present work was to decide which of the two models can be derived from the vacancy hopping mechanism with an attractive potential between the dopant and the vacancy.
On the other hand, the point-defect gradient term has a non-negligible influence on the simulation of dopant diffusion when the vacancy gradients are large as, e.g., during transient diffusion after ion implantation.

2. Description of the Applied Method

The atomistic basis for the calculation of the dopant and vacancy fluxes is the vacancy hopping model. The only movement allowed is a vacancy hopping to a nearest neighbour site thus exchanging its place with either a silicon atom or the dopant atom. The probability of such a transition per time (the jump rate) may depend on the distance between the vacancy and the dopant atom thus taking into account some kind of force between the defect and the dopant. Special cases are, e.g., tracer diffusion where all jump frequencies are equal or the model of Hu [3] with 4 different jump frequencies which has been used to estimate the correlation factor for impurity diffusion via vacancies. For the calculation shown in this work, 7 different jump rates have been used taking into account interactions up to the 3rd coordination site. The method applied deals with a statistical ensemble of a limited, three-dimensional area of a silicon crystal which is represented by a time dependent two-particle probability distribution. $c(i,j,t)$ is the probability that the dopant atom is at site i and the vacancy is at site j. Since interactions of more than 2 particles are neglected, c contains all information about the statistical ensemble. Therefore the one-particle profiles as well as the dopant and vacancy fluxes can be calculated from the two-particle probability at each time. At the onset of diffusion, the correlated probability $c(i,j,0)$ is set to the product of the one-particle distributions $d(i,0)$ for the dopant and $v(j,0)$ for the vacancy. This corresponds to a statistical independence of dopant and vacancy distribution. Then the Master equation for the correlated probability $c(i,j,t)$ is solved to get the time evolution of $c(i,j,t)$. The boundary condition is particle conserving for the dopant, for the vacancy a constant flux at the surfaces can be simulated which prevents the vacancy gradient from flattening out too fast. The time evolution of $c(i,j,t)$ corresponds to a relaxation of the system towards a local equilibrium within a time scale which is small compared to the time necessary to get a major change in the 1-particle profiles $d(i,t)$ and $v(j,t)$. When the local equilibrium has been reached, transport coefficients can be calculated by dividing the fluxes through the corresponding driving forces (gradients).
The Master equation is solved numerically using an explicit timestep scheme with a stepsize of $0.1\ \frac{1}{\tau}$ (τ is the jump frequency of a free vacancy).

3. Applications and Results

The method outlined in the previous section has been applied to the open question of diffusion theories adressed in the introduction. Calculations have been performed

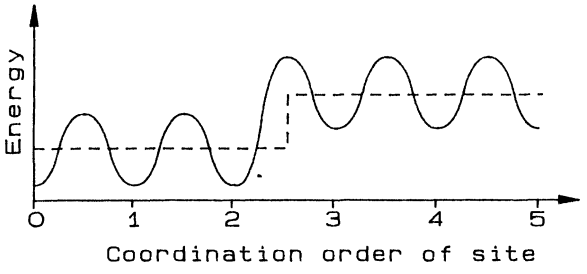

Figure 1: Schematic diagram of the vacancy potential as a function of distance from the impurity atom at the origin. The dashed line indicates the potential well caused by the impurity.

on a simulation area of 7 lattice constants in the x- and y-direction and 8 lattice constants in the z-direction (3136 sites) with different attractive potentials. For the sake of simplicity, rectangular potential wells are assumed. Fig. 1 shows the schematic drawing of a potential well reaching to the 2nd nearest neighbour site. Calculations have also been performed for a potential range up to the 1st and 3rd coordination site, and without a potential well (tracer diffusion).

Jump frequencies have been scaled to the jump frequency τ of a free vacancy, the lattice constant a (5.431$\AA$) was used as unit for lengths. This means that fluxes are given in units of τ/a^2, diffusion coefficients in $\tau \cdot a^2$, time in $\frac{1}{\tau}$, and densities in $1/a^3$. The initial conditions were a homogenous dopant profile of $2.5 \cdot 10^{-3} \cdot \frac{1}{a^3}$ and a constant vacancy gradient of $6.6 \cdot 10^{-4} \cdot \frac{1}{a^4}$ in the z-direction (the values result from a normalization condition). The constant surface vacancy flux was $6 \cdot 10^{-5} \cdot \frac{\tau}{a^2}$. This was chosen so that the vacancy profile changes as little as possible and the equilibrium establishes as fast as possible. All jump frequencies were set to τ except for the one which leads out of the potential well which was set to $\tau_{esc} = 0.02 \cdot \tau$. Thus, the

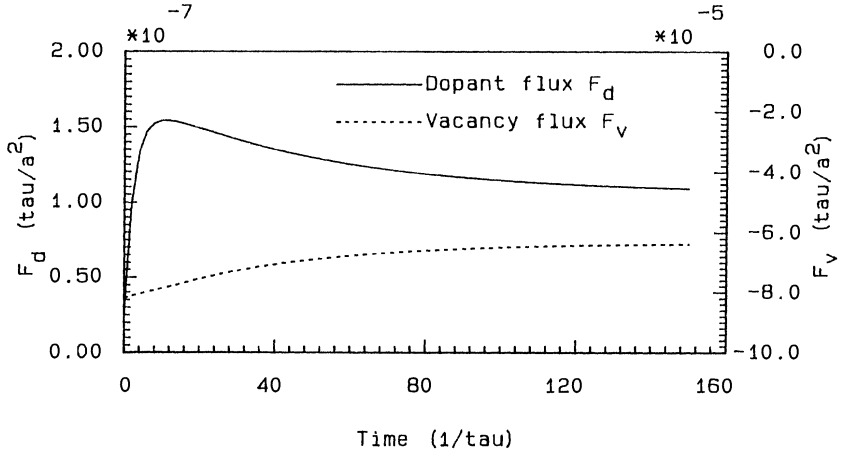

Figure 2: Evolution of dopant and vacancy fluxes with time for an attractive potential ending at the 2nd coordination site.

probability for the pair to dissociate was 50 times smaller than for staying together. Fluxes and diffusion coefficients are evaluated at a site in the center of the calculation area.

Fig. 2 shows the results for a potential range up to the 2nd coordination site. Local equilibrium is established after about 60 $\frac{1}{\tau}$. The absolute value of the dopant flux in the equilibrium is larger than at $t = 0$ due to the higher probability of a vacancy staying at neighbouring sites after the formation of pairs. The direction is opposite to the vacancy flux. In Fig. 3, the underlying potential ranges up to the 3rd coordination site. Due to the larger radius of the pairs, the time required for local equlibrium to establish is longer (about 120 $\frac{1}{\tau}$). At about $t = 20\frac{1}{\tau}$, the sign of the dopant flux changes, both fluxes are now in the same direction corresponding to the predictions of pair diffusion theories. The absolute value of $\underline{F_d}$ is also increased due to the larger vacancy density around the dopant.

The vacancy gradient stays constant throughout the calculation to within 10 percent. Table 1 lists the results for the vacancy diffusion coefficient D_v and the normalized dopant transport coefficient $T_d^o = \alpha \cdot D_d^o$. The errors are estimated from variations at sites around the centre. Notice that for tracer diffusion random walk theory can be

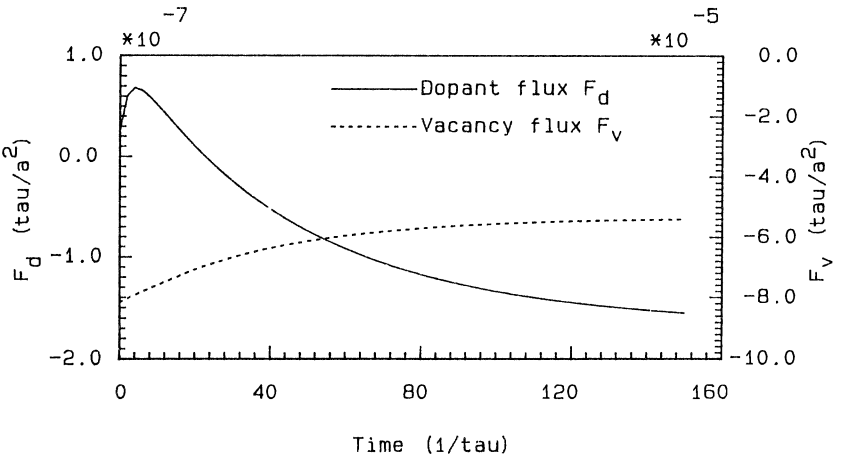

Figure 3: Evolution of dopant and vacancy fluxes with time for an attractive potential ending at the 3rd coordination site.

Table 1: Diffusion and transport coefficients

potential range		no potential	1st coo. site	2nd coo. site	3rd coo. site
D_v	$[\tau \cdot a^2]$	0.120 +/- 0.008	0.113 +/- 0.007	0.101 +/- 0.006	0.079 +/- 0.012
T_d^o	$[\tau \cdot a^2]$	-0.120 +/- 0.007	-0.300 +/- 0.015	-0.541 +/- 0.03	0.715 +/- 0.30

used to calculate the exact values $D_v^{trac} = -T_d^{o,trac} = 0.125\tau \cdot a^2$. As table 1 shows, D_v is reduced with increasing potential range due to the increasing probability for the vacancy to be bound to the dopant.

4. Conclusion

Dopant transport coefficients for diffusion under vacancy gradients have been calculated on the basis of the vacancy hopping mechanism with different binding potentials between dopant and vacancy. The results of this work show that both, pair diffusion models [1] and the theory of Maser [2], can be explained with the vacancy hopping mechanism, depending only on the type of interaction potential.

5. Acknowledgments

We wish to thank Dr. E. Geissler and H. Krausenberger from the RRZE (regional computation centre Erlangen) for their help with the adaption of the program used to a CRAY-YMP and a CDC4680. This work was part of **ADEQUAT** (JESSI project BT1B) and was funded as ESPRIT project 7236.

References

[1] M. Orlowsky, Appl. Phys. Lett. 53, 1323 (1988)

[2] K. Maser, Experimentelle Technik der Physik 39, 169 (1991)

[3] S. M. Hu, Phys. Rev. 180, 773 (1969)